The Journal of Immunology

Delays and Diversions Mark the Development of B Cell Responses to *Borrelia burgdorferi* Infection

Christine J. Hastey, Rebecca A. Elsner, Stephen W. Barthold and Nicole Baumgarth

J Immunol published online 30 April 2012
http://www.jimmunol.org/content/early/2012/04/30/jimmunol.1103735

The Journal of Immunology is published twice each month by The American Association of Immunologists, Inc., 1451 Rockville Pike, Suite 650, Rockville, MD 20852

Print ISSN: 0022-1767 Online ISSN: 1550-6606.

Published April 30, 2012, doi:10.4049/jimmunol.1103735

Delays and Diversions Mark the Development of B Cell Responses to *Borrelia burgdorferi* Infection

Christine J. Hastey, Rebecca A. Elsner, Stephen W. Barthold, and Nicole Baumgarth

B cell responses modulate disease during infection with *Borrelia burgdorferi*, the causative agent of Lyme disease, but are unable to clear the infection. Previous studies have demonstrated that *B. burgdorferi* infection induces predominantly T-independent B cell responses, potentially explaining some of these findings. However, others have shown effects of T cells on the isotype profile and the magnitude of the *B. burgdorferi*-specific Abs. This study aimed to further investigate the humoral response to *B. burgdorferi* and its degree of T cell dependence, with the ultimate goal of elucidating the mechanisms underlying the failure of effective immunity to this emerging infectious disease agent. Our study identifies distinct stages in the B cell response using a mouse model, all marked by the generation of unusually strong and persistent T-dependent and T-independent IgM Abs. The initial phase is dominated by a strong T-independent accumulation of B cells in lymph nodes and the induction of specific Abs in the absence of germinal centers. A second phase begins around week 2.5 to 3, in which relatively short-lived germinal centers develop in lymph nodes, despite a lymph node architecture that lacks clearly demarcated T and B cell zones. This response failed, however, to generate appreciable numbers of long-lived bone marrow plasma cells. Finally, there is a slow accumulation of long-lived Ab-secreting plasma cells in bone marrow, reflected by a strong but ultimately ineffective serum Ab response. Overall, the study indicates that *B. burgdorferi* might evade B cell immunity by interfering with its response kinetics and quality. *The Journal of Immunology*, 2012, 188: 000–000.

Lyme borreliosis, caused by the spirochete *Borrelia burgdorferi* and transmitted via *Ixodes* spp. ticks, is the most common arthropod-borne illness in the United States and Europe (1, 2). Disease manifestations of acute Lyme borreliosis include flu-like symptoms, often accompanied by erythema migrans at the site of the tick bite, and regional lymphadenopathy (3, 4). We recently developed a mouse model of infection with host-adapted *B. burgdorferi* spirochetes that closely mimics the clinical course of tick-borne infection and can serve as a model for studies on disease progression and immune response development (5). Later-stage Lyme borreliosis often involves the neurologic system, carditis, and/or arthritis, manifestations that undergo bouts of sporadic remission during persistent infection (3). Immunocompetent hosts living in endemic areas can be reinfected (6, 7), indicating a lack of functional immune-mediated memory responses. The mechanism underlying this lack of a functional adaptive memory response has not been determined.

The importance of the adaptive immune system in controlling the disease manifestations, but not the infection itself, has been demonstrated in previous studies (8–10). *B. burgdorferi*-infected SCID and RAG$^{-/-}$ mice, lacking both B and T cells, have persistent and severe arthritis without spontaneous remission. B cells seem to be primarily responsible for control of disease progression and resolution observed in wild-type mice, as B cell deficiency resulted in more severe disease, whereas T cell deficiency had little impact on arthritis resolution and the development of other inflammatory disease manifestations in C57BL/6 mice (10). In fact, adoptive transfer of CD4$^+$ T cells into RAG$^{-/-}$ mice prior to *B. burgdorferi* infection increased arthritis and carditis severity, and CD8$^+$ T cell transfer increased arthritis severity (11).

The role of T cells in the generation of protective B cell responses to *B. burgdorferi* infection is insufficiently explored. Mice deficient in CD40L generated Abs that conferred passive protection, and immune sera from T cell-deficient mice were as protective as control sera (12). In contrast, serum Ab responses to both *B. burgdorferi* lysate and one of its Ags, decorin binding protein A (DbpA), showed greatly reduced titers and changes in their Ab isotype profile in CD40L$^{-/-}$ compared with wild-type mice (10). Thus, although T cell-independent Ab appears sufficient for protection, T cells can amplify and regulate the quality of the *B. burgdorferi*-specific Ab response. Support for a role of *B. burgdorferi*-specific Abs in B cell-mediated disease resolution comes from studies showing that passive transfer of serum from infected, but not naive, immune-competent mice results in arthritis and carditis resolution in SCID mice (13). Despite this Ab-mediated resolution of disease, spirochetes persist in tissues, indicating a profound lack of effectiveness of Abs in removal of tissue-resident *B. burgdorferi*.

High titers of *B. burgdorferi*-specific Ab responses against *B. burgdorferi* lysates can be found in the serum of infected humans (14) and in experimentally infected animal models, including mice (15). Notably, passive transfer of immune serum from infected mice to naive mice protected against later *B. burgdorferi* challenge (15). Using serial serum dilutions to titrate protective activity, the protective capacity of serum from persistently infected mice was shown to be transient, peaking at day 30 and decreasing thereafter,

Graduate Group in Microbiology, University of California, Davis, Davis, CA 95616; and Center for Comparative Medicine, University of California, Davis, Davis, CA 95616

Received for publication December 21, 2011. Accepted for publication March 29, 2012.

This work was supported in part by National Institutes of Health/National Institute of Allergy and Infectious Diseases Grant AI073911 (to N.B. and S.W.B.) and T32 Training Grant AI060555 (to C.J.H. and R.A.E.).

Address correspondence and reprint requests to Dr. Nicole Baumgarth, Center for Comparative Medicine, University of California, Davis, One Shields Avenue, Davis, CA 95616. E-mail address: nbaumgarth@ucdavis.edu

Abbreviations used in this article: Arp, arthritis related protein; ASC, Ab-secreting cell; BmpA, *Borrelia* membrane protein A; DbpA, decorin binding protein A; OspC, outer surface protein C; PNA, peanut agglutinin; qPCR, quantitative PCR; qRT-PCR, quantitative RT-PCR; T_{FH}, T follicular helper; WT, wild-type.

whereas *Borrelia* Ab responses to *B. burgdorferi* lysate continued to increase over time (15). These studies point to shifts in quality of the B cell response to *B. burgdorferi* over time that are not effectively captured by measurement of serum Ab levels to *B. burgdorferi* lysate alone. Furthermore, they indicate an ongoing dynamic interaction between the host adaptive immune system and the spirochetes in long-term *B. burgdorferi*-infected hosts that ultimately benefits the spirochete, enabling establishment of persistent infections.

This study aimed to explore the dynamics of the B cell response to *B. burgdorferi* infection and to determine the extent to which CD4 T cells regulate this response. Using a previously developed mouse model that closely mimics tick-borne *B. burgdorferi* infection (5), we demonstrate unique characteristics of the B cell response over the course of infection, indicating multiple points at which the infection appears to delay, divert, and alter effective B cell responses to this pathogen.

Materials and Methods

Borrelia burgdorferi

A clonal strain of *B. burgdorferi* sensu stricto (cN40) was grown in modified Barbour–Stoenner–Kelley II medium (16) at 33˚C and enumerated with a Petroff–Hauser bacterial counting chamber (Baxter Scientific, McGaw Park, IL) for inoculation of SCID mice.

Mice and infections

Eight- to twelve-week-old female or male C57BL/6J (B6), C57BL/6.CB17-*Prkdc*^{scid}/SzJ (SCID), CD40L-deficient B6.129S2-*Cd40lg*^{tm1Imx}/J (CD40L$^{-/-}$), and ICOS-deficient B6.129P2-*Icos*^{tm1Mak}/J (ICOS$^{-/-}$) mice were obtained from The Jackson Laboratory. BALB/cAnNHsd (BALB/c) were obtained from Harlan Laboratories. Breeding pairs of B6.129SvEv-SAP$^{-/-}$ (SAP$^{-/-}$) mice were a generous gift of Pamela Schwartzberg (17). All mice were maintained in microisolator cages and kept under conventional housing conditions.

Mice were infected with tissue-adapted spirochetes by transfer of ear tissue from SCID mice, infected for at least 14 d, into the right hind leg under skin of recipients as described previously (5) or received transfer of uninfected ear tissue from SCID mice (sham infection). To compare responses in the gene-targeted mice to those of wild-type (WT) control mice, WT mice were analyzed simultaneously in each experiment to account for any differences introduced by the infection with *B. burgdorferi*-infected tissues. To generate *B. burgdorferi*-infected tissue for transplantation, SCID mice were infected via s.c. injections with 10^4 *B. burgdorferi*. Infected SCID mice were euthanized, and ear tissues were cleaned with 70% ethanol and diluted Nolvasan (Pfizer) before removal. Lateral tail vein blood collections were performed to obtain serum. For influenza infection, BALB/c mice were infected intranasally under isoflurane anesthesia with a sublethal dose of A/PR/8 (H1N1) corresponding to 10 PFU in 40 μl PBS per mouse. Virus was grown in embryonated hen eggs, and PFUs were established as described (18). Mice were euthanized by overexposure to carbon dioxide. All studies were conducted according to protocols approved by the University of California, Davis, Animal Use and Care Committee.

CD4 T depletion

B6 mice were given i.p. either 0.3 mg anti-CD4 (GK1.5) mAb, purified from tissue culture supernatants via protein G affinity chromatography, or polyclonal rat isotype control Ab (Sigma) on day −3. On days 0 and 6, mice were given an additional dose of 0.1 mg of respective Abs. Two mice from each group were euthanized at day 0, and spleens and right inguinal lymph nodes were collected to confirm CD4 T cell depletion by FACS analysis using anti-CD4 (RM4.5) Ab. Quantification of CD4 T cells was also performed on spleens and right inguinal lymph nodes at day 10 postinfection. Analysis showed that anti-CD4 depletion removed >99.5% of CD4 T cells in those tissues.

Flow cytometry

Single-cell suspensions from inguinal lymph nodes and spleens were stained as previously described (5). Briefly, after Fc receptor blocking, the following Ab conjugations were used at predetermined concentrations: CXCR5–biotin, CD11a–Cy7PE, CD138–PE (all BD Pharmingen), CD4–Alexa 750 (RM4.5), CD3e–biotin, CD44–allophycocyanin, ICOS–PE, CD19–Cy5PE, CD3–allophycocyanin Efluor 780 (all eBioscience), CD4–FITC (GK1.5), CD8a–Cy5.5PE, CD38–PE, CD24–Cy5PE (all in-house generated), and streptavidin–Qdot605 (Invitrogen). CXCR5–biotin staining was performed first at 37˚C for 30 min, and the subsequent steps were performed on ice for 20 min. Dead cells were identified by staining with live/dead violet stain (Invitrogen by Life Technologies) on ice for 30 min. Data acquisition was performed on a 13-color FACSAria instrument (BD Biosciences) (19). Data were analyzed using FlowJo software (kind gift from Adam Treister).

Histology and immunofluorescence

Lymph nodes were fixed in neutral buffered formalin, embedded in paraffin, sectioned at 4 μm thickness, and then stained with H&E. Other lymph nodes were frozen on dry ice in Tissue-Tek OCT (Sakura) and stored at −80˚C until sectioned. Five-micrometer sections were cut on a Leica cryostat and dried onto Superfrost/Plus slides (Fisher Scientific) at room temperature overnight. Slides were fixed for 10 min in ice-cold acetone, dried for 1 h, rehydrated in PBS plus 0.1% BSA, pH 7.2, for 30 min, and nonspecific staining was blocked with immunofluorescence staining buffer (PBS plus 0.1% BSA plus 1% normal horse serum). Sections were stained with anti-CD4–Efluor 450 (RM4-5; eBioscience) and either peanut agglutinin (PNA)–biotin (Vector Labs) or CD45R–biotin (in-house generated) in immunofluorescence staining buffer at room temperature for 2 h. Slides were washed twice in PBS and once in PBS plus 0.1% BSA for 5 min each and stained with anti-IgD–FITC (in-house generated) and streptavidin–Alexa Fluor 594 (Invitrogen) in immunofluorescence staining buffer for 1 h. Slides were washed three times in PBS and mounted with Fluoromount-G (Southern Biotech). Images were collected on an Olympus BX61 microscope with an Olympus DP72 color camera and were processed with MetaMorph (Molecular Devices) and ImageJ (National Institutes of Health) software.

ELISPOT assay and ELISA

To probe for *B. burgdorferi*-specific Ab-producing cells, 96-well plates (Multiscreen HA filtration; Millipore) were coated overnight with four immune prevalent recombinant *B. burgdorferi* proteins all generated based on the N40 sequence, 1 μg/ml DbpA and 2 μg/ml each for outer surface protein C (OspC), arthritis related protein (Arp), and *Borrelia* membrane protein A (BmpA) or *B. burgdorferi* lysate (Fig. 4G) in PBS, generated as previously described (5). We previously established their relative seroreactivity after *B. burgdorferi* infection. Furthermore, measurement of each of those protein-specific Ab responses showed higher Ab titers than measurement of serum against *B. burgdorferi* lysate generated by sonication from culture-grown *B. burgdorferi*. Presumably, this is because the antigenic nature of culture-grown *B. burgdorferi* is distinct from that of spirochetes in mammalian hosts (5). In addition both anti-DbpA and anti-OspC responses can provide passive immune protection, and anti-Arp Abs have arthritis-resolving capacity (20). For influenza-specific ELISPOT assays, plates were coated with 2000 HAU/ml influenza A/PR8 (18). After blocking with 4% BSA in PBS, cell suspensions in medium (RPMI 1640, 292 μg/ml L-glutamine, 100 μg/ml penicillin and streptomycin, 10% heat-inactivated FCS, and 0.03 M 2-mercaptoethanol) were placed in the starting well and 2-fold serially diluted. Cells were incubated at 37˚C overnight then lysed with water. Ab binding was revealed by adding biotin-conjugated anti-IgM (Southern Biotech) or anti-IgH+L (Southern Biotech) in 2% BSA in PBS for 2 h, followed by streptavidin-HRP incubation (Vector Laboratories) in 2% BSA in PBS for 1 h and revealing with 3-amino-9-ethylcarbazole (Sigma-Aldrich) for 10 min. Plates were dried, and mean spots were counted in all wells with visible spots using a stereomicroscope. Mean numbers ± SD were calculated from cell counts of all wells with countable spots.

B. burgdorferi-specific ELISAs were performed by coating 96-well plates (Maxisorb; Thermo Fisher Scientific) with four recombinant *B. burgdorferi* proteins as for ELISPOT assay in PBS overnight. Influenza-specific ELISAs were performed by coating 96-well plates (Maxisorb; Thermo Fisher Scientific) with sucrose-gradient purified A/PR8 virus as for ELISPOT assay in PBS overnight. After blocking with PBS/1% heat-inactivated calf serum/0.1% milk powder/0.05%Tween 20 for 1 h, serially diluted serum was added to the plates for 2 h. Plates were washed, and Ab binding was revealed using biotin-conjugated anti-IgG (Southern Biotech) followed by a streptavidin-HRP (Vector Laboratories) incubation for 1 h and then substrate (10 mg/ml 3,3′5,5′-tetramethylbenzidine in 0.05 mM citric acid, 3% hydrogen peroxide) for 20 min. Reactions were stopped with 1 N sulfuric acid, and absorbance was read at 450 nm and reference wavelength of 595 nm using a SpectraMax M5 (Molecular Devices). Relative units Ab levels were calculated by comparison with a day 60

immune serum from mice-infected host-adapted spirochetes titrated on the same plates or hyperimmune serum from mice infected with A/PR8.

Adoptive transfer of bone marrow Ab-secreting cells

Femoral bone marrow from naive B6 mice ($n = 4$), day 168 *B. burgdorferi*-infected B6 mice ($n = 5$), or day 504 A/PR8-infected BALB/c mice ($n = 4$) was prepared into single-cell suspensions. Naive non-irradiated B6 or BALB/c mice received i.v. 2×10^7 cells. The number of Ab-secreting cells (ASC) was determined by ELISPOT assay prior to transfer. A control group ($n = 4$) received 2×10^7 femoral bone marrow cells from uninfected mice. To ensure that *B. burgdorferi* was not transferred with donor bone marrow, heart, spleen, and urinary bladder were tested by quantitative PCR (qPCR) in recipient mice, and all were found to be negative for *B. burgdorferi*.

qPCR

qPCR was used to detect *B. burgdorferi flagellin* (*flaB*) DNA in draining activated lymph node, as previously described (21). All samples were assayed with positive and negative controls. DNA was extracted from tissues with DNeasy kits (Qiagen, Valencia, CA) according to the manufacturer's instructions. Prior to DNA extraction, tissue samples were weighed. Data are expressed as the number of DNA copies per milligram of tissue.

Quantitative RT-PCR low-density array

Inguinal lymph nodes from mice infected via tissue transplant at days 0, 10, and 22 were collected and kept frozen at −80°C until processing. Total RNA was extracted by the RNeasy Mini Kit (Qiagen) according to the manufacturer's instructions. First-strand cDNA was synthesized from total RNA using the QuantiTect Reverse Transcription Kit (Qiagen) in 50-μl reactions according to the manufacturer's instructions. The preamplification reaction was done via activation at 95° for 15 s, amplification for 25 cycles at 95°C for 15 s, 55°C for 15 s, and 70°C for 45 s, followed by elongation at 70°C for 5 min. Preamplified products were diluted 1:10 and used as templates for qPCR analysis. All samples were analyzed for the presence of 18S rRNA to determine the efficiency of the nucleic acid extraction and amplification.

The synthesized cDNA template from each sample (30 μl) was added to 50 μl of 2× Universal PCR Master Mix (Applied Biosystems) in 100-μl reaction mixtures. The mixture was added to each line of a micro fluidic low-density array card (Applied Biosystems) and amplified using an ABI Prism 7900HT sequence detection system (Applied Biosystems): 2 min at 50°C to 10 min at 94.5°C, followed by 40 cycles of denaturation at 97°C for 30 s, and annealing and extension at 59.7°C for 1 min.

Primers and probes were designed using Primer Express software (Applied Biosystems). The amplification efficiency (E) of all assays was calculated from the slope of a standard curve generated on a 10-fold dilution in triplicate for every cDNA sample using the formula $E = 10^{(-1/\text{slope})} - 1$. Detection limits were ~10 copies of cDNA per reaction. The coefficient of variability for qPCR was 15% or less when determined for 10 replicates. As a reference gene to normalized transcriptional activity of mouse cytokines, mouse GAPDH was used.

Results

Lack of CD4 T cell accumulation in lymph node after B. burgdorferi *infection*

Regional lymphadenopathy is a common sign of infection with *B. burgdorferi* and is successfully mimicked in our mouse model using tissue-adapted spirochetes for infection (5). Our previous study showed that increased lymph node cellularity shortly postinfection was attributable in large part to the accumulation of $CD19^+$ B cells, some of which contributed *B. burgdorferi*-specific Abs, but not T cells. This led us to analyze more closely the activation of CD4 T cells in the lymph nodes of *B. burgdorferi*-infected mice. To determine the extent to which CD4 T cells are activated and contribute to the regulation of *B. burgdorferi*-specific B cell responses, we first conducted a time-course analysis on single-cell suspensions from the draining right inguinal lymph nodes, assessing frequencies of $CD19^+$ B cells and $CD4^+$ and $CD8^+$ T cells by flow cytometry at intervals for 60 d after *B. burgdorferi* infection. Consistent with our previous report, total lymph node cellularity rapidly increased by 400%, peaking at day 10 postinfection (Fig. 1A). Throughout the infection, this increase was due primarily to $CD19^+$ B cells, whereas $CD4^+$ and $CD8^+$ T cell numbers did not change significantly (Fig. 1A). As a consequence, the ratio of $CD19^+$ B cells to $CD4^+$ T cells increased in the lymph nodes, with increasing numbers of B cells per CD4 T cell at early time points, peaking at day 10 (Fig. 1B). That ratio stayed elevated through day 60. Additionally, the phenotype of the B cells was determined by flow cytometry, and it was found that the majority of the B cells were naive $IgD^+CD45R^+CD23^+$ (Fig. 1D). To determine the impact of tissue transfer alone on the local immune response, inguinal lymph nodes from mice that received ear tissue from infected or uninfected (sham) SCID mice 10 d prior were analyzed by flow cytometry. *B. burgdorferi*-infected mice showed a strong increase in B cell frequencies (Fig. 1E), whereas sham-infected mice had frequencies of B and T cells that were similar to those of non-infected and non-transplanted mice (data not shown). Marked differences were observed also for the lymph node cellularity (data not shown).

Immunofluorescence on lymph nodes at 10 d postinfection (Fig. 1C) confirmed these findings, demonstrating that the vast majority of lymph node cells were B cells as seen in the low magnification image of the whole lymph node (Fig. 1C, *left panel*). B cells appeared tightly packed throughout the lymph node, which lacked the typical follicular arrangement. CD4 T cells were scattered, lacking discernible T cell zones in both $CD45R^{hi}$ (B cell) and $CD45R^{lo}$ (plasma blast) areas of the lymph node (Fig. 1C, *middle* and *right panels*). Consistent with the lower cell yield, lymph nodes from mice that received sham tissue were smaller (Fig. 1F) than those from infected mice (Fig. 1G). Thus, *B. burgdorferi* infection induces a rapid and drastic increase in lymph node B cell numbers and destruction of B and T cell zones in the absence of concomitant or even moderate increases in CD4 T cells numbers over at least 60 d.

Presence of activated CD4 T cells after B. burgdorferi *infection*

The unusually high B/T ratio might suggest that CD4 T cells were not activated upon infection with *B. burgdorferi*, explaining previous evidence for the T cell-independence of the *B. burgdorferi*-specific B cell responses. To examine this further, we determined the frequency of activated CD4 T cells and/or T follicular helper (T_{FH}) cells in inguinal lymph nodes draining the site of infection. Activated CD4 T cells were identified as being $CD11a^{hi}$ and $CD44^{hi}$ by flow cytometry (Fig. 2A) (22). Activated T cells started to appear on day 8 after *B. burgdorferi* infection and remained increased through day 28. T_{FH} cells, important for supporting germinal center B cell responses, were also consistently found by staining for CXCR5 and ICOS (23–26). The frequency of T_{FH} cells increased until day 15 and then declined rapidly. Consistent with the presence of activated T cells and T_{FH} cells, cytokine mRNA levels for IL-4 and IL-21 and less so IL-2, crucial cytokines for T-dependent B cell responses (27), were increased on days 10 and 22 compared with those of day 0 (Fig. 2B), whereas IFN-γ mRNA levels were unaffected. These data indicate that although overall T cell numbers do not significantly increase in lymph nodes of *B. burgdorferi*-infected mice, transient and short-lived CD4 T cell activation and differentiation to T_{FH} nonetheless occurred.

CD19 accumulation in lymph nodes is T cell independent

We showed previously that the unusually large accumulation of B cells in the lymph nodes of *B. burgdorferi*-infected mice (Fig. 1) is correlated with the appearance of live, and not heat-killed, *B.*

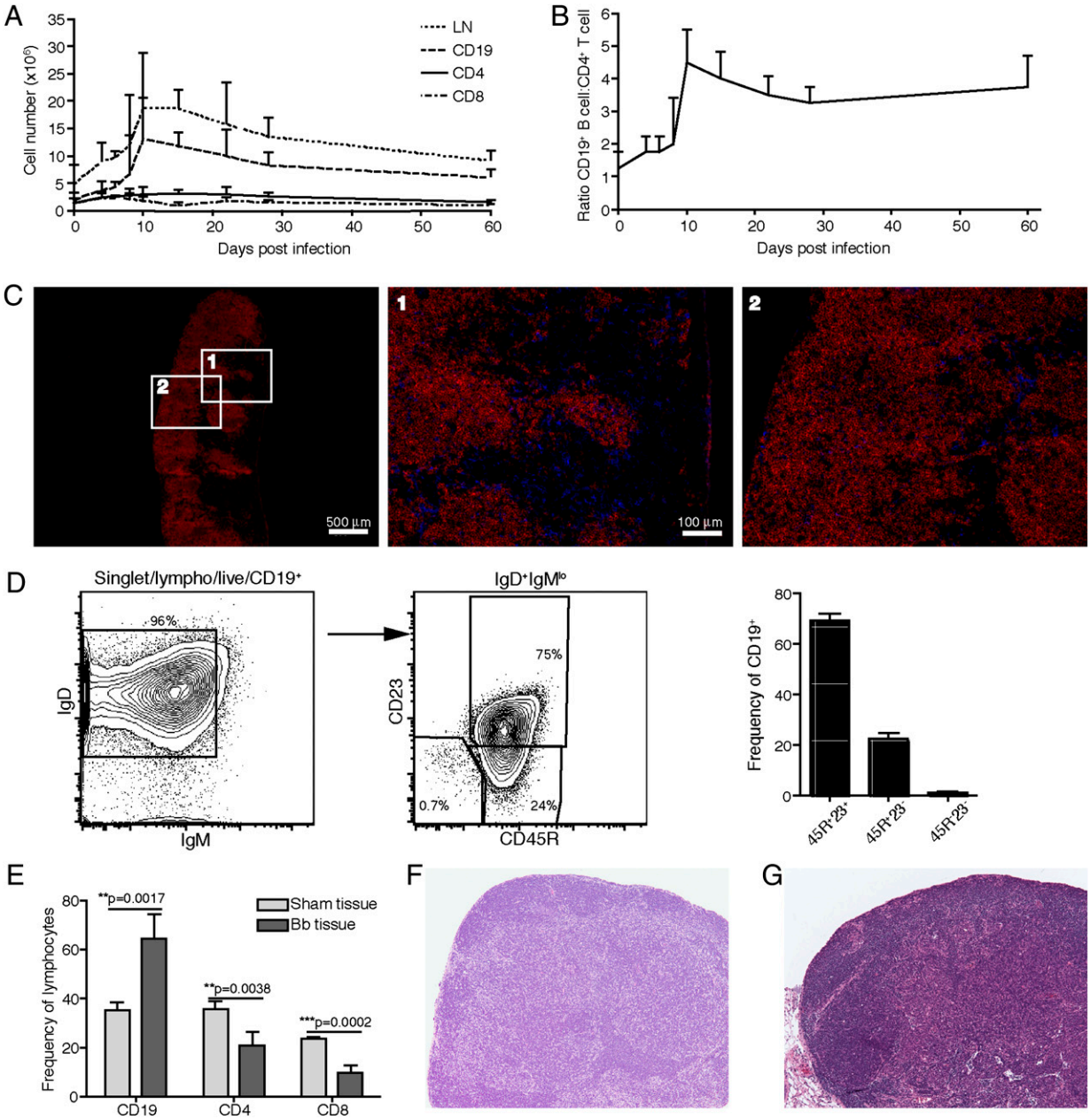

FIGURE 1. B cell but not T cell accumulation in regional lymph nodes after *B. burgdorferi* infection. B6 mice were infected with host-adapted spirochetes via tissue transplant of *B. burgdorferi*-infected tissue from *B. burgdorferi*-infected SCID mice into the right leg. At indicated times postinfection, right inguinal lymph nodes were collected, and cellularity was assessed with a hemocytometer after trypan blue exclusion. Total lymph node (LN), $CD19^+$ B cell, $CD4^+$ T cell, and $CD8^+$ T cell frequencies were determined by flow cytometry. (**A**) Line graph indicates mean cell count for each indicated cell population ($n = 4$), error bars represent SD. (**B**) Shown are the ratios of $CD19^+$ B cell per $CD4^+$ T cell, as assessed from numbers shown in (A). Line graph indicates mean values, error bars represent SD. (**C**) Two-color immunofluorescence identifies the $CD45R^+$ (red) B cells and $CD4^+$ (blue) T cells in the lymph node on day 10 postinfection. *Middle* (*1*) and *right* (*2*) *panels* are higher magnification images of the *left panel*, as indicated. Scale bars indicate magnification. (**D**) Shown are representative 5% contour plots with outliers of $CD19^+$ B cells from lymph nodes of day 10 infected mice after gating of (single cells/live/lymphocyte gate/$CD19^+$). *Left panel*, Naive cells are identified as IgD^+ IgM^{lo}. *Middle panel*, Further gating of naive cells identified as $CD23^{hi}$ $CD45R^+$. (**E**) Frequencies of $CD19^+$ B cells, $CD4^+$ T cells, and $CD8^+$ T cells as assessed by flow cytometry in draining lymph nodes from day 10 after transplant of infected or uninfected (sham) tissue. Bars represent the mean of the group; error bars represent SD ($n = 4$/group). (**F** and **G**) H&E staining on day 10 after transplant of uninfected (sham) tissue (F) or infected tissue (G), representative of $n = 2$. Original magnification ×10.

burgdorferi in the lymph nodes but is independent of MyD88 signaling (5) and thus unlikely a result of TLR-mediated mitogenic B cell responses to *B. burgdorferi*. To determine whether the B cell accumulation is reliant on T cell costimulation, lymph node cellularity and cellular compositions were assessed in mice lacking the $CD4^+$ T cell costimulatory molecules CD40L, ICOS, and SAP on day 10 postinfection, the peak of the lymph node cellularity in WT mice. Lack of these costimulatory molecules, or indeed the depletion of all CD4 T cells via injection with anti-CD4, had no significant effect on total lymph node cellularity (Fig. 3A) or B cell numbers (Fig. 3B) compared with WT B6 mice. B6-*Tcr*$\gamma\delta^{-/-}$ mice deficient in γδ T cells also failed to show any effects of γδ T cells on lymph node cellularity or $CD19^+$ B cell numbers at day 10 postinfection (data not shown). Thus, the rapid B cell accumulation characterizing the early lymph node response to *B. burgdorferi* infection occurs independently of T cells.

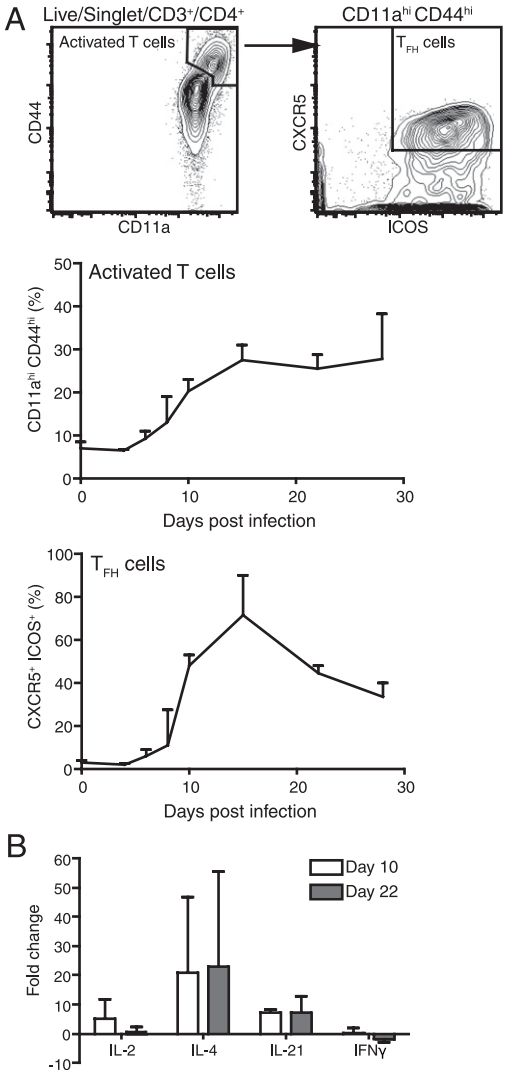

FIGURE 2. CD4 T cells are activated in regional lymph nodes after *B. burgdorferi* infection. (**A**) Shown are representative 5% contour plots with outliers of CD4 T cells from lymph nodes of day 10 infected mice after gating of $CD4^+$ T cells (single cells/live/$CD19^-/CD3^+$). *Left panel*, Activated T cells are identified as $CD11a^{hi}$ $CD44^{hi}$. *Right panel*, Activated $CD4^+$ T cells; CXCR5 and ICOS expression identifies T_{FH} cells. Frequencies of activated T cells (*middle panel*) and T_{FH} cells (*bottom panel*) among $CD44^{hi}$ $CD11a^{hi}$ CD4 T cells at indicated times postinfection with *B. burgdorferi*. Data represent the mean of the group + SD ($n = 4$). (**B**) Shown are mean relative expression levels + SD of T cell cytokines measured by qRT-PCR of lymph nodes of mice infected for 10 or 22 d compared with lymph nodes from uninfected mice ($n = 4$). Data are normalized for RNA input by using the housekeeping gene GAPDH.

Effects of T cells on B. burgdorferi*-specific Ab production*

We previously concluded that the induction of Abs against *B. burgdorferi* in the draining lymph node was specific and furthermore showed that it was unaffected by the lack of MyD88 signaling (5). However, it is currently unclear to what extent the B cell Ab response is dependent on T cells or T cell-expressed costimulatory molecules. In contrast to the T cell-independent accumulation of B cells in affected lymph nodes after *B. burgdorferi* infection, previous studies reported that the absence of T cells or CD40L affects the magnitude of the *B. burgdorferi*-specific serum Ab responses and changes their Ig isotype profiles (10, 12), suggesting that Ab production and B cell accumulation are two independently regulated processes. Indeed, although B cell accumulation was not affected, the presence of CD4 T cells and the expression of the costimulatory molecules CD40L, ICOS, and SAP affected maximal Ab responses in the lymph nodes of *B. burgdorferi*-infected mice (Fig. 3C–E). Mice depleted of CD4 T cells or mice lacking SAP showed significant reductions in frequencies of $CD138^+$ lymph node plasma cells by flow cytometry (Fig. 3C), as well as *B. burgdorferi*-specific IgM (Fig. 3D) and IgG ASC (Fig. 3E) on day 10 of infection compared with WT controls assayed at the same time. $CD40L^{-/-}$ mice also showed reduced IgM and IgG ASC but had similar levels of $CD138^+$ plasma cells by flow cytometry. Notably, the lack of ICOS had no effect on plasma cell development or early Ab production in response to *B. burgdorferi* infection. The observed enhancing effects of T cells on the *B. burgdorferi*-specific B cell responses are likely acting on extrafollicular foci cells, as these are strongly induced on day 10 after *B. burgdorferi* infection, whereas germinal centers are just beginning to form (Fig. 4A) (5). Notably, and consistent with earlier studies (28, 29), the number of IgM ASC was higher than the IgG ASC in the WT mice, indicating a strong low-affinity Ab response early in *B. burgdorferi* infection. Like the IgG response, however, CD4 T cells clearly enhanced the IgM response.

We also compared the Ig responses in the spleen of *B. burgdorferi*-infected compared with sham-infected mice and found no significant responses in the spleen (Fig. 4G). This is consistent with our previous report in which we failed to find increased cellularity or Ab production in the spleen after *B. burgdorferi* infection (5). Thus, CD4 T cells engage with B cells in a CD40L- and SAP-dependent but ICOS-independent manner to enhance early *B. burgdorferi*-specific Ab responses in lymph nodes of *B. burgdorferi*-infected mice.

Induction of transient germinal center B cell responses after B. burgdorferi *infection*

The dominance of T-dependent and T-independent *B. burgdorferi*-specific IgM secretion (Fig. 3D), the transient nature of the lymph node T_{FH} cells (Fig. 2A), and the destruction of the lymph node architecture (Fig. 1C) suggested that *B. burgdorferi*-infected mice might be unable to develop strong T-dependent germinal centers and thereby might lack long-lived plasma cells and memory responses. To assess the kinetics and magnitude of the germinal center response, flow cytometry was used to identify lymph node germinal center B cells as $CD19^+$ $CD38^{lo}$ $CD24^{hi}$ (Fig. 4A) and PNA^+ (data not shown) in WT mice over a period of 60 d after *B. burgdorferi* infection. The analysis showed that germinal center B cells were first detected between days 8 and 10 (Fig. 4A). Their numbers peaked around day 15, whereas their frequencies increased for about another week. Thereafter, germinal center B cells rapidly decreased (Fig. 4A). By immunofluorescence, PNA-stained germinal centers were detectable but sparse at day 10, but readily detectable between days 15 and 21 (Fig. 4B), consistent with the flow cytometry data, and then disappeared by about day 28 of infection. Lymph node histology on day 28 further showed that the lymph nodes had lost many of their cells and appeared "empty" and "exhausted" (Fig. 4C). Responses in other lymph nodes were similar to those of the draining lymph nodes but were delayed by up to 2 wk. These lymph nodes had similar Ab response qualities, measured by IgG and IgM ELISPOT assay, but their responses were smaller than that of the draining lymph node (data not shown).

Overall, the kinetics of germinal center B cells closely followed that of the T_{FH} cell population (Fig. 2A), appearing somewhat slow in induction and very rapid in decline. Lack of Ag presence cannot explain the rapid decline of the germinal center responses, as *B. burgdorferi* DNA was detectable in the lymph nodes by

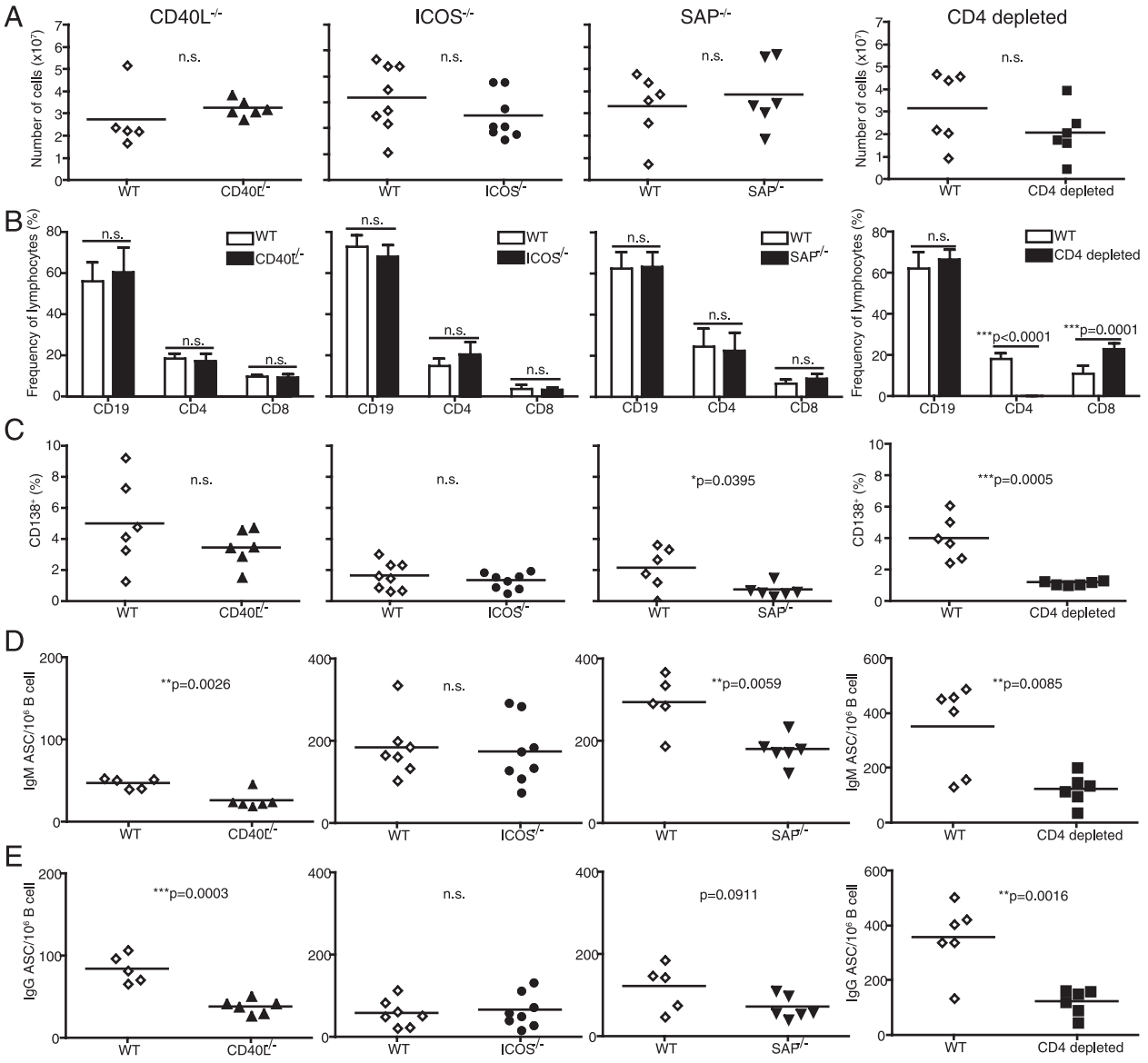

FIGURE 3. CD4 T cells play a role in B cell differentiation but not B cell expansion in lymph nodes. Data are pooled from two independent studies. Shown are scatterplots, each symbol representing one animal; line indicates the mean of the group (n = 8/group). (**A**) Draining lymph node cellularity in indicated knockout mice compared with WT (B6) mice or in mice depleted of CD4 T cells via Ab treatment prior to infection with tissue adapted spirochetes. (**B**) Frequencies of $CD19^+$ B cells, $CD4^+$ T cells, and $CD8^+$ T cells as assessed by flow cytometry. Bars represent the mean of the group; error bars represent SD (n = 8/group). Statistical analysis was conducted with Student t test. (**C**) $CD138^+$ plasma cell frequencies in CD4-depleted mice and in mice deficient in CD40L, ICOS, or SAP on day 10 of *B. burgdorferi* infection compared with WT (B6) controls. Cells were gated as $CD138^+$ (after gating of live/lymphocytes/singlet/$CD4^-CD8^-$). (**D**) Frequencies of IgM and (**E**) IgG-secreting cells as assessed by ELISPOT assay with a pool of *B. burgdorferi* recombinant proteins (DbpA, Arp, OspC, and BmpA) on day 10 of infection in right inguinal lymph nodes from CD4-depleted, $CD40L^{-/-}$, $ICOS^{-/-}$, and $SAP^{-/-}$ mice. Data are pooled from at least two independent experiments.

qPCR for at least 120 d postinfection (Fig. 4F), and live *B. burgdorferi* can be cultured from the lymph nodes for at least 90 d (5).

As expected, depletion of CD4 T cells caused a significant reduction in germinal center B cells, as did the absence of $CD40L^{-/-}$ and $SAP^{-/-}$ mice (Fig. 4D). Mice that lacked ICOS showed no significant decrease in the small numbers of germinal center B cells countable on day 10 compared with WT mice, but they did so by day 15 (Fig. 4E). Taken together, the data indicate that the lymph nodes are sites of transient, short-lived T cell-dependent germinal center B cell responses that show a relatively late start compared with immunization studies where germinal centers can be seen as early as day 4 after Ag application, for example with tetanus toxin (30) and also acute viral infections. They also seem to disappear rather rapidly between days 21 and 28. On the basis of the histology, the data further indicate that the lymph node might be unable to sustain germinal center responses at this time point, despite the presence of *B. burgdorferi* Ag.

Presence of IgM and IgG ASC in bone marrow from long-term infected mice

Because of the transient nature of the germinal center response after *B. burgdorferi* infection, we asked whether the germinal centers that do form are functional by studying long-lived plasma cell generation. As expected, serum Ab levels to *B. burgdorferi* were clearly maintained long-term in infected animals (Fig. 5A). ELISPOT analysis on single-cell suspensions from bone marrow at various times postinfection with *B. burgdorferi* revealed that bone marrow plasma cells accumulated very slowly and with distinct

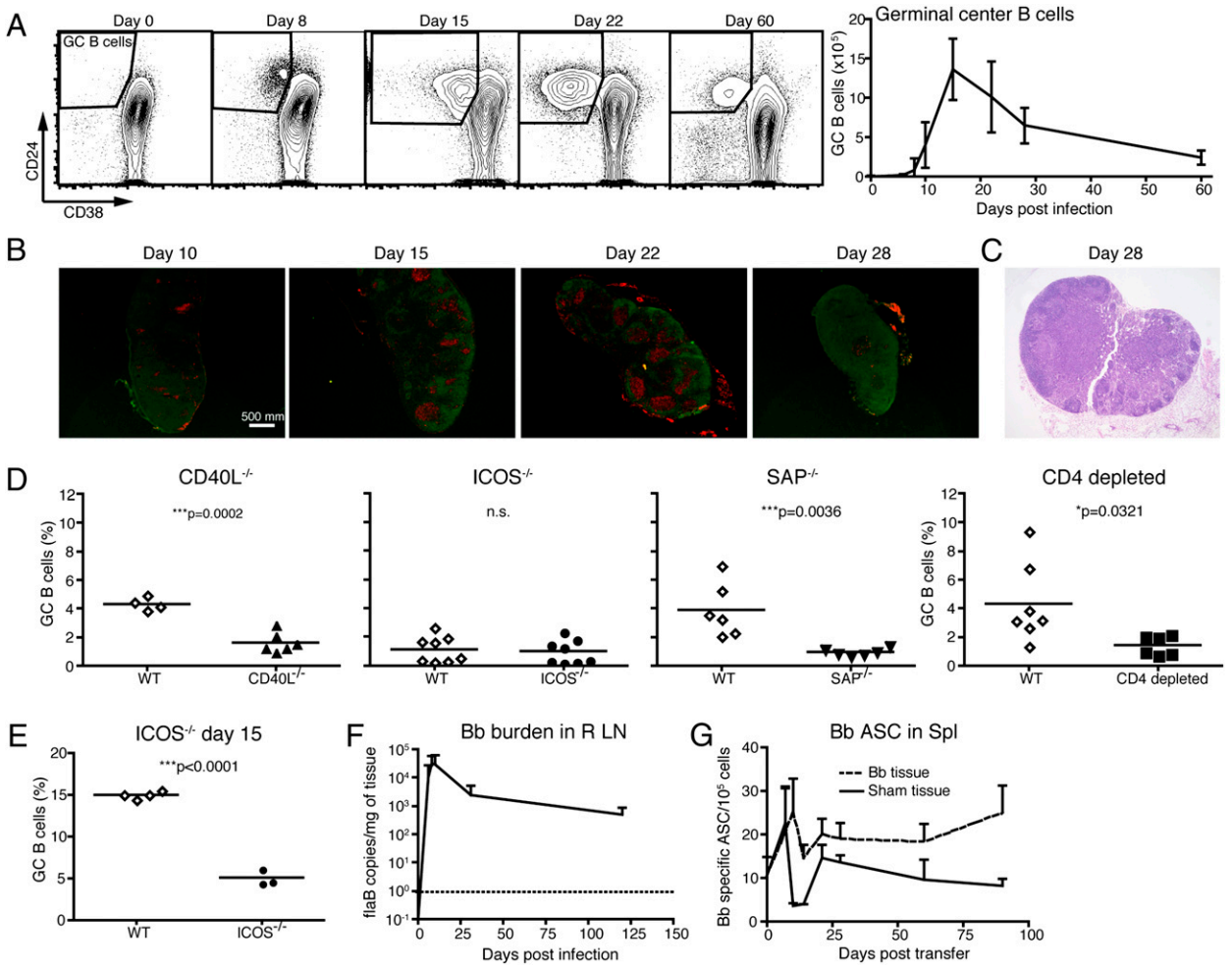

FIGURE 4. Induction of transient germinal center B cell responses after *B. burgdorferi* infection. (**A**) Shown are representative 5% contour plots and outliers from FACS data taken at indicated times postinfection; right inguinal lymph nodes were collected, and nine-color flow cytometry was used to determine the frequency of germinal center B cells ($CD38^{lo}$ $CD24^{hi}$) after gating of $CD4^-CD8^-$ $CD19^+$ cells (singlet/live). Data are representative of two independent experiments. Germinal center B cell frequencies are summarized as a line graph showing the mean and SD of the group ($n = 4$). (**B**) Two-color immunofluorescence identifies the PNA^+ (red) germinal center B cells and IgD^+ (green) B cells in the lymph node on day 10, 15, 22, and 28 postinfection. (**C**) H&E staining on day 28 postinfection (original magnification ×4), representative of $n = 2$. (**D**) Shown are scatterplots of germinal center B cell frequencies, identified as $CD38^{lo}$ $CD24^{hi}$, assessed by flow cytometry in CD4-depleted, $CD40L^{-/-}$, $ICOS^{-/-}$, and $SAP^{-/-}$ mice on day 10 of infection. Each symbol represents one animal; line indicates the mean of the group ($n = 8$). (**E**) Shown are scatterplots as in (C) of germinal center B cell frequencies of $ICOS^{-/-}$ mice on day 15 of infection. Data are representative of two independent experiments, except the ICOS data on day 15, which were done once. (**F**) *B. burgdorferi* burden as determined by qRT-PCR measuring *flaB* DNA copy numbers per milligram of lymph node tissue is summarized as a line graph showing the mean and SD of the group ($n = 4$). (**G**) Frequencies of ASC in the spleen after transfer of either infected SCID tissue or sham uninfected tissue as determined by ELISPOT coated with *B. burgdorferi* lysate. Line graph indicates the mean and SD of the group of pooled spleens analyzed in triplicate dilution series ($n = 3$).

kinetics compared with the rapid serum Ab response (Fig. 5A). Given that lymph node germinal centers were gone by about day 28 of infection, but significant accumulation of ASC secreting various IgG isotypes and IgM required >60 d (Fig. 5B–E), the data indicate that the lymph node responses are not significant sources for the bone marrow plasma cell accumulation, which seem to be induced later. Notably, we found a strong IgM ASC response in the bone marrow consistent with the high levels of specific serum IgM. IgG1, a predominantly T-dependent isotype found after many bacterial infections, was not measured, as previous studies had shown negligible IgG1 responses to *B. burgdorferi* infection in C57BL/6 mice (5).

To test the extent to which the *B. burgdorferi*-specific bone marrow ASC are T cell dependent and therefore likely to be germinal center-derived, we collected bone marrow from $CD40L^{-/-}$ and WT mice on day 105 after *B. burgdorferi* infection. Numbers of IgM, IgG2b, and IgG2c ASC were significantly decreased in the $CD40L^{-/-}$ mice (Fig. 6A–C) compared with WT mice, whereas IgG3 was not significantly affected by the loss of CD40L (Fig. 6D). These data suggest that most of the bone marrow-derived plasma cells were generated in a T-dependent manner and thus likely the result of germinal center responses.

Finally, to test whether the plasma cells found in mice infected for greater than 100 d are in fact long-lived, we conducted adoptive transfer experiments. For that, naive mice received bone marrow containing 5.6×10^5 *B. burgdorferi*-specific ASC from day 168 chronically *B. burgdorferi* infected mice, as determined by ELISPOT analysis at the time of transfer. In contrast to control mice that received bone marrow from non-infected mice and which did not show significantly increased *B. burgdorferi*-specific Ab responses, serum from the *B. burgdorferi*-infected recipient mice showed significant levels of *B. burgdorferi*-specific Abs for

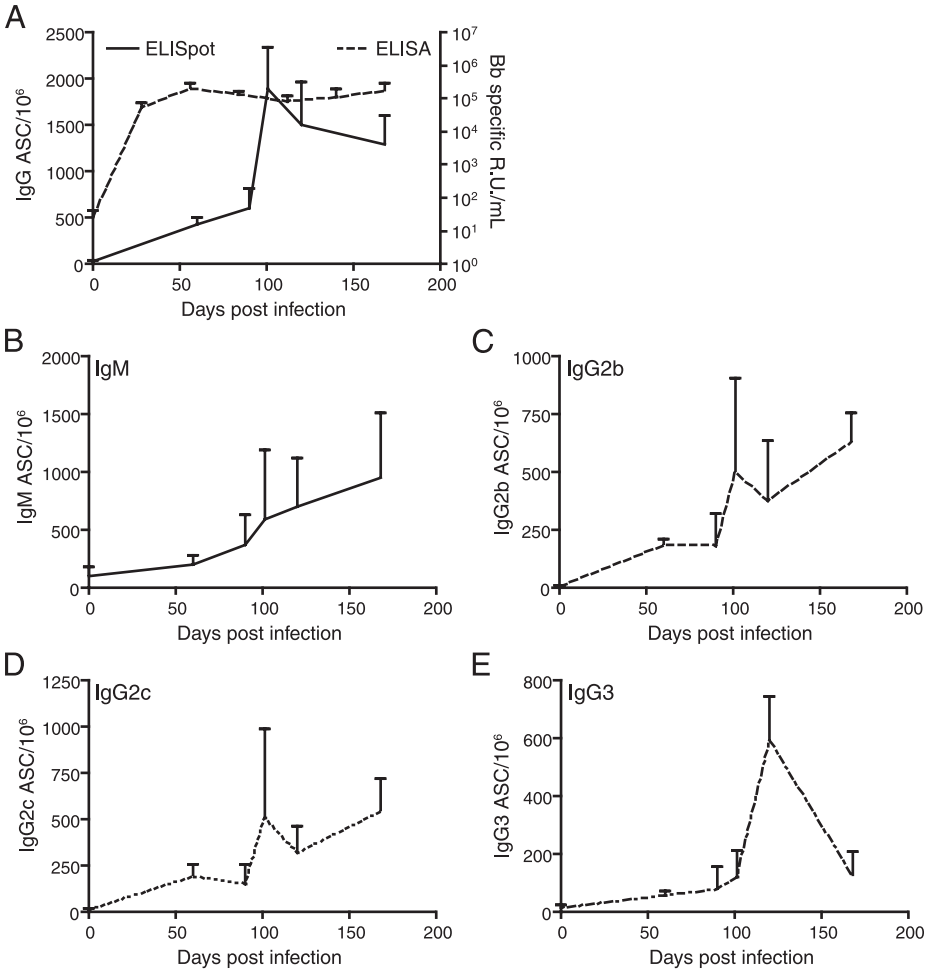

FIGURE 5. Presence of ASC in bone marrow from long-term infected mice. At indicated times postinfection, femurs were collected from mice, and bone marrow was assessed for ASC. (**A**) Sum of IgG isotype-secreting bone marrow ASC (Fig. 6C–E). Serum was collected, and *B. burgdorferi*-specific IgG was measured at indicated points postinfection. Line graph indicates mean of group with error bars representing SD (n = 5). Shown are frequencies of (**B**) IgM-, (**C**) IgG2b-, (**D**) IgG2c-, and (**E**) IgG3-secreting cells per 10^6 cells as assessed by ELISPOT assay with a pool of recombinant *B. burgdorferi* proteins (DbpA, Arp, OspC, and BmpA). Line indicates mean of group with error bars representing SD (n = 5). Data from days 90, 100, and 120 were combined from two independent experiments, n = 4/group.

>100 d (Fig. 6E). The kinetics of the Ab titers were overall similar to that of control mice that received bone marrow, containing 3.25×10^4 A/PR8-specific ASC, from long-term (day 504 postinfection) influenza-infected mice (Fig. 6E), which induces strong long-lived Ab responses (31). Thus, *B. burgdorferi* infection induces long-lived bone marrow plasma cell responses to the four recombinant immune prevalent Ags evaluated, but with kinetics that makes it unlikely that they are derived from the responses in the draining lymph nodes. Given that the other lymph nodes became involved no later than 2 wk after the draining lymph node (Ref. 5 and data not shown) and that in our model the spleen does not appear to be involved (Fig. 4G and Ref. 5), they may also not be derived from responses in secondary lymphoid tissues.

Discussion

The Ab response to *B. burgdorferi* infection is the only known adaptive immune mechanism that ameliorates disease and provides immune protection. However, it is of insufficient quality to clear the infection. This suggests that *B. burgdorferi* might subvert the B cell response to avoid removal from the host to fulfill its life cycle, which includes transmission to another host via uptake by its vector, the *Ixodes* tick. In this study, we provide evidence that *B. burgdorferi* infection indeed alters normal B cell response development in the lymph nodes in multiple ways. First, B cells rapidly and strongly accumulate in regional lymph nodes in response to the presence of live *B. burgdorferi*, but independent of either MyD88 signaling (5) or T cell help (Figs. 1, 3). Although some lymph node B cells rapidly differentiated to Ab-producing cells, they failed to mount strong T-dependent B cell responses and formed only transient germinal centers. The outcome is a B cell response that is dominated by IgM-secreting cells, both induced early in the lymph nodes and also found later in the bone marrow, and the presence of IgG responses in which only ~50% of the response is clearly T-dependent (Fig. 3) and which does not appear to contribute significantly to the long-term Ab responses in the bone marrow. Long-lived *B. burgdorferi*-specific IgG-secreting plasma cells accumulated only slowly in the bone marrow (Fig. 6). Together, these data provide strong evidence for the diversion and delay of B cell responses by *B. burgdorferi*, which might help *B. burgdorferi* to establish and maintain persistence.

The possible effects of the extensive accumulation of the mainly naive B cells (Fig. 1C) on the ability of the lymph nodes to induce and sustain adaptive immune responses remain to be studied. It is tempting to speculate that the changes in B/T ratios together with the loss of clearly demarcated T and B cell zones might reduce the efficiency with which T-dependent B cell responses and germinal center responses are induced, given the intricate nature and chemokine-mediated migration of T and B cells that regulates their interactions in secondary lymphoid organs (32, 33). Notably, studies by others showed that *B. burgdorferi* infection causes an overexpression of the follicle-homing chemokine CXCL13 in *B. burgdorferi*-infected tissues (34). Given the fact that passive transfer of serum Abs from mice infected for 2 mo can protect from challenge with *B. burgdorferi* (15), the same serum is unable to clear an infected host. Even relatively minor delays in induction of protective Ab responses might play a role in allowing *B. burgdorferi* to evade immunity by rapidly and widely disseminating in an infected host (35).

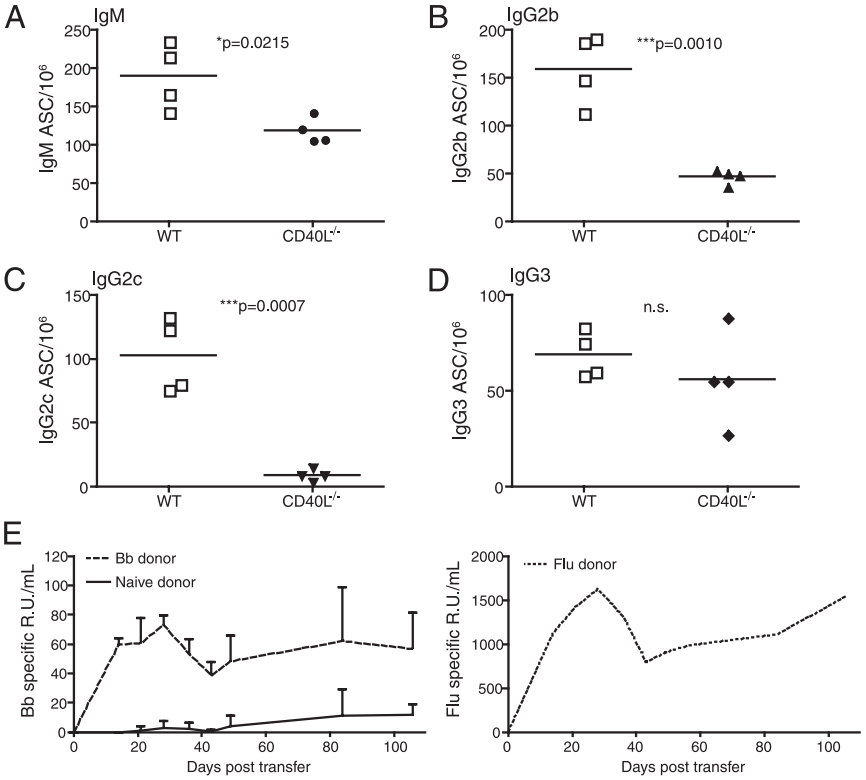

FIGURE 6. Presence of T cell-dependent long-lived plasma cells in the bone marrow after *B. burgdorferi* infection. Shown are *B. burgdorferi*-specific (**A**) IgM-, (**B**) IgG2b-, (**C**) IgG2c-, and (**D**) IgG3-secreting cells per 10^6 cells as assessed by ELISPOT assay from C57BL/6J or CD40L$^{-/-}$ mice at day 105 post-infection. Symbols represent data from individual mice; line indicates mean values (n = 4/group). (**E**) Ag-specific serum Ab levels from recipient mice after transfer of bone marrow from day 168 *B. burgdorferi*-infected mice (n = 4), naive mice (n = 4), or day 504 flu A/PR8-infected mice (n = 2), as assessed by ELISA coated with *B. burgdorferi* recombinant proteins (DbpA, Arp, OspC, and BmpA) or purified influenza virus. Lines indicate mean of groups, error bars SD. Relative units Ab were calculated in comparison with a relevant hyperimmune serum.

The overabundance of lymph node B cells and loss of tissue architecture early in infection might also be involved in the rapid shutdown of the germinal center responses in those tissues. Our data demonstrating a strong early induction of CD4 T cell activation and their differentiation to cells with a T_{FH} phenotype (Fig. 2) suggest that there is no defect in T cell activation, but rather that there is a failure to maintain T-dependent germinal center responses. Mechanisms that remain to be explored could include *B. burgdorferi* infection-induced changes in the stromal environment of the lymph node, which might result in reduced or altered production of critical cytokines, such as CCR7 and CXCL13 and the B cell survival factor BAFF (36), or an increase in uptake of such factors by the large numbers of B cells present in the lymph nodes, among others.

Some strains of *B. burgdorferi* contain a variable-major protein-like sequence expressed lipoprotein (*vlsE*) in their genome, which they use to vary their antigenic surface coat (37), which may enable immune escape via antigenic shift. However, the genome of the strain used for the current study, N40, expresses a truncated form of *vlsE* (GenBank accession no. PRJNA29357; http://www.ncbi.nlm.nih.gov/genome?term=PRJNA29357), and N40-infected animals do not mount a serum response to the conserved internal C6 peptide of vlsE from either N40 or from the prototype C6 derived from B31 (data not shown). To survey antigenic shift early in infection, we performed a quantitative RT-PCR (qRT-PCR) low-density array that screens 43 known *B. burgdorferi* genes between day 10 (low germinal center response) and day 22 (robust germinal center response) but found very little change in gene expression (data not shown). However, these data may mask potential protein expression changes or changes of the subcellular location of *B. burgdorferi*-expressed proteins (38). On the basis of these data, we would reason that *B. burgdorferi* immune evasion may not be due only to antigenic shifts, such as those observed on *Borrelia hermsii* (39). In support, earlier studies demonstrate furthermore that mice infected with *B. burgdorferi* for 90 d and then treated with antibiotics were protected from challenge with *B. burgdorferi* isolates (or infected skin tissue) taken from day 180-infected mice, thus arguing against a simple switch-away from protective Ab responses (40). On the basis of the presented study, we propose that the herein uncovered alterations in the B cell responses to *B. burgdorferi* contribute to its persistence in an immunocompetent host. However, a more detailed analysis of the antigenic nature of *B. burgdorferi* in the mammalian host and the specificity of the Abs generated is clearly needed but hampered currently by the lack of techniques to isolate sufficient quantities of *B. burgdorferi* grown in tissue of infected mammalian hosts that reflect the in vivo Ag repertoire.

One of the most striking features of the B cell response to *B. burgdorferi* infection is the ongoing dominance of the T-dependent and T-independent IgM response, both early in the lymph nodes (5) and later in the bone marrow (Fig. 5). Whether this is the result of *B. burgdorferi*-mediated immune diversion or a result of the type of B cell or Ag to which the Abs are raised remains to be determined. Long-term IgM-producing cells have recently been shown to provide protection against intracellular infections and in response to challenge after immunization with polysaccharides (41–44). IgM has also been shown to contribute to protection from death and the lowering of West Nile virus burden in the blood (45). Furthermore, the pentameric structure and flexibility of IgM allows higher avidity binding to bacterial surface Ags than monomeric IgG (46) and may be useful in protection from extracellular pathogens. Thus, IgM may facilitate clearance of *B. burgdorferi* from the bloodstream, and potentially the blood-filtering spleen, where it is found only during short episodic periods (35). However, IgM may be less effective in supporting bacterial clearance from the skin and other tissues. Because of its large size, IgM might not be able to reach *B. burgdorferi* in the tissues in the absence of inflammation and the resulting increase in vascular leakage. In contrast to infection with pathogens that are circulating in the blood, such as *B. hermsii*, the

unusually strong and sustained IgM response may be overall detrimental for the host and represent a failure of B cells to undergo class-switch recombination to an IgG response that could be more effective in clearance of *B. burgdorferi* residing in various tissues.

Studies by Bockenstedt and colleagues (47) indicated that marginal zone B cells might be activated in response to infection with culture-grown *B. burgdorferi*. Marginal zone B cells are known to differentiate rapidly to IgM-producing cells in response to blood-derived Ags (32). However, we do not see an early involvement of the spleen in our infection model (Ref. 5 and Fig. 4G). Previous studies suggested that splenic involvement after *B. burgdorferi* infection depends on the site of infection (48). That study showed that inoculation at the shoulder resulted in doubling of the number of splenocytes by day 14, whereas inoculation into the footpad never resulted in enhanced splenocyte numbers. Our animal model uses infection into the right hind leg, which we show in this study to be associated with an increase in lymphocytes in the regional lymph nodes. Consistent with the study by de Souza et al. (48), it does not result in increased splenocyte numbers (5). Thus, the splenic response does not appear to contribute significantly in *B. burgdorferi*-specific B cell responses in the model used here.

Responses by B-1b cells, a source for natural IgM (49), are induced to *B. hermsii* infection, the causative agent of relapsing fever, a blood-borne disease (50, 51). However, *B. burgdorferi* is only found in the blood during acute stages of infection, and intermittently thereafter, in the immunocompetent laboratory mouse (9, 35), and our preliminary studies do not support induction of B-1 cells as a strong contributor to the *B. burgdorferi*-induced IgM response in lymph nodes (C.J. Hastey, R.A. Elsner, S.W. Barthold, and N. Baumgarth, unpublished observations). Similarly, perisinusoidal B-2 cells in the bone marrow were shown to respond to blood-borne microbes by producing Ag-specific IgM in a T-independent manner (52) and are therefore unlikely a source for *B. burgdorferi* infection-induced IgM. Together with our studies showing that a good fraction of the IgM response in both lymph nodes and bone marrow is T-dependent (Fig. 3), it appears most likely that the ongoing IgM production is a result of a non-class-switched B-2 cell response. The data thereby suggest that *B. burgdorferi* might interfere with the processes underlying efficient class-switch recombination of B cells.

The generation of long-lived plasma cells in *B. burgdorferi*-infected mice was surprising, given the short-lived nature of the lymph node germinal center responses and their distinct kinetics. As discussed above and reported previously (5), the spleen is involved little in generation of Abs to *B. burgdorferi* infection in our model, and although *B. burgdorferi* is readily cultured from lymph nodes, the spleen is culture positive only late in infection (5), raising the question of what tissue is the source of the accumulating long-lived plasma cells. Given the slow kinetics, it is possible that ectopic germinal centers, which often form after *B. burgdorferi* infection in the nervous system (34) and in the vicinity of arthritic joints and other tissue (35, 53), might be a major source for these cells.

To what extent these long-lived plasma cells contribute to immune protection remains to be studied; however, they might be of relative little protective value. This is because previous studies demonstrated that whereas serum from mice infected with *B. burgdorferi* for 60 d can provide passive immune protection, serum from long-term infected mice loses this capacity (15). Our studies now show that bone marrow plasma cells are not present until after the maximum protective capacity of the serum is reached. Memory B cells arrive through the same germinal center responses as long-lived plasma cells. Therefore, our data indicate that memory to *B. burgdorferi* infection may also not be formed until late during infection. Given that most patients are treated early during Lyme borreliosis, shortly after a tick bite and the appearance of the characteristic skin rash, early antibiotic treatment that eliminates infection may prevent the development of long-term plasma cell responses and memory B cell formation. This is consistent with the susceptibility to reinfection observed in individuals living in *B. burgdorferi*-endemic areas (6, 54).

Collectively, our study provides evidence for a complex interplay between *B. burgdorferi* with the host B cell immune arm that affects the B cell response at multiple stages, ultimately failing to allow clearance of the pathogen but sufficient to suppress pathogen burden and disease manifestations.

Acknowledgments

We thank Stefan Tunev for the spleen data in Fig. 4, Edlin Escobar for expert technical help, Abigail Spinner for help in operating the BD FACSAria, Emir Hodzic for expertise and analysis of the qRT-PCR, Pam Schwartzberg (National Institutes of Health) for SAP$^{-/-}$ mice, and Adam Treister (Tree Star) for FlowJo software.

Disclosures

The authors have no financial conflicts of interest.

References

1. Bacon, R. M., K. J. Kugeler, and P. S. Mead; Centers for Disease Control and Prevention (CDC). 2008. Surveillance for Lyme disease—United States, 1992-2006. *MMWR Surveill. Summ.* 57: 1–9.
2. Hubálek, Z. 2009. Epidemiology of lyme borreliosis. *Curr. Probl. Dermatol.* 37: 31–50.
3. Steere, A. C. 1989. Lyme disease. *N. Engl. J. Med.* 321: 586–596.
4. Steere, A. C. 2001. Lyme disease. *N. Engl. J. Med.* 345: 115–125.
5. Tunev, S. S., C. J. Hastey, E. Hodzic, S. Feng, S. W. Barthold, and N. Baumgarth. 2011. Lymphoadenopathy during lyme borreliosis is caused by spirochete migration-induced specific B cell activation. *PLoS Pathog.* 7: e1002066.
6. Nowakowski, J., I. Schwartz, R. B. Nadelman, D. Liveris, M. Aguero-Rosenfeld, and G. P. Wormser. 1997. Culture-confirmed infection and reinfection with *Borrelia burgdorferi*. *Ann. Intern. Med.* 127: 130–132.
7. Piesman, J., M. C. Dolan, C. M. Happ, B. J. Luft, S. E. Rooney, T. N. Mather, and W. T. Golde. 1997. Duration of immunity to reinfection with tick-transmitted *Borrelia burgdorferi* in naturally infected mice. *Infect. Immun.* 65: 4043–4047.
8. Schaible, U. E., M. D. Kramer, C. Museteanu, G. Zimmer, H. Mossmann, and M. M. Simon. 1989. The severe combined immunodeficiency (scid) mouse. A laboratory model for the analysis of Lyme arthritis and carditis. *J. Exp. Med.* 170: 1427–1432.
9. Barthold, S. W., C. L. Sidman, and A. L. Smith. 1992. Lyme borreliosis in genetically resistant and susceptible mice with severe combined immunodeficiency. *Am. J. Trop. Med. Hyg.* 47: 605–613.
10. McKisic, M. D., and S. W. Barthold. 2000. T-cell-independent responses to *Borrelia burgdorferi* are critical for protective immunity and resolution of lyme disease. *Infect. Immun.* 68: 5190–5197.
11. McKisic, M. D., W. L. Redmond, and S. W. Barthold. 2000. Cutting edge: T cell-mediated pathology in murine Lyme borreliosis. *J. Immunol.* 164: 6096–6099.
12. Fikrig, E., S. W. Barthold, M. Chen, I. S. Grewal, J. Craft, and R. A. Flavell. 1996. Protective antibodies in murine Lyme disease arise independently of CD40 ligand. *J. Immunol.* 157: 1–3.
13. Barthold, S. W., S. Feng, L. K. Bockenstedt, E. Fikrig, and K. Feen. 1997. Protective and arthritis-resolving activity in sera of mice infected with *Borrelia burgdorferi*. *Clin. Infect. Dis.* 25(Suppl 1): S9–S17.
14. Aguero-Rosenfeld, M. E., J. Nowakowski, S. Bittker, D. Cooper, R. B. Nadelman, and G. P. Wormser. 1996. Evolution of the serologic response to *Borrelia burgdorferi* in treated patients with culture-confirmed erythema migrans. *J. Clin. Microbiol.* 34: 1–9.
15. Barthold, S. W., and L. K. Bockenstedt. 1993. Passive immunizing activity of sera from mice infected with *Borrelia burgdorferi*. *Infect. Immun.* 61: 4696–4702.
16. Barbour, A. G. 1984. Isolation and cultivation of Lyme disease spirochetes. *Yale J. Biol. Med.* 57: 521–525.
17. Czar, M. J., E. N. Kersh, L. A. Mijares, G. Lanier, J. Lewis, G. Yap, A. Chen, A. Sher, C. S. Duckett, R. Ahmed, and P. L. Schwartzberg. 2001. Altered lymphocyte responses and cytokine production in mice deficient in the X-linked lymphoproliferative disease gene SH2D1A/DSHP/SAP. *Proc. Natl. Acad. Sci. USA* 98: 7449–7454.
18. Doucett, V. P., W. Gerhard, K. Owler, D. Curry, L. Brown, and N. Baumgarth. 2005. Enumeration and characterization of virus-specific B cells by multicolor flow cytometry. *J. Immunol. Methods* 303: 40–52.

19. Rothaeusler, K., and N. Baumgarth. 2006. Evaluation of intranuclear BrdU detection procedures for use in multicolor flow cytometry. *Cytometry A* 69: 249–259.
20. Feng, S., E. Hodzic, K. Freet, and S. W. Barthold. 2003. Immunogenicity of *Borrelia burgdorferi* arthritis-related protein. *Infect. Immun.* 71: 7211–7214.
21. Hodzic, E., S. Feng, K. J. Freet, and S. W. Barthold. 2003. *Borrelia burgdorferi* population dynamics and prototype gene expression during infection of immunocompetent and immunodeficient mice. *Infect. Immun.* 71: 5042–5055.
22. Baumgarth, N., M. Egerton, and A. Kelso. 1997. Activated T cells from draining lymph nodes and an effector site differ in their responses to TCR stimulation. *J. Immunol.* 159: 1182–1191.
23. Schaerli, P., K. Willimann, A. B. Lang, M. Lipp, P. Loetscher, and B. Moser. 2000. CXC chemokine receptor 5 expression defines follicular homing T cells with B cell helper function. *J. Exp. Med.* 192: 1553–1562.
24. Breitfeld, D., L. Ohl, E. Kremmer, J. Ellwart, F. Sallusto, M. Lipp, and R. Förster. 2000. Follicular B helper T cells express CXC chemokine receptor 5, localize to B cell follicles, and support immunoglobulin production. *J. Exp. Med.* 192: 1545–1552.
25. Hutloff, A., A. M. Dittrich, K. C. Beier, B. Eljaschewitsch, R. Kraft, I. Anagnostopoulos, and R. A. Kroczek. 1999. ICOS is an inducible T-cell costimulator structurally and functionally related to CD28. *Nature* 397: 263–266.
26. Ansel, K. M., L. J. McHeyzer-Williams, V. N. Ngo, M. G. McHeyzer-Williams, and J. G. Cyster. 1999. In vivo-activated CD4 T cells upregulate CXC chemokine receptor 5 and reprogram their response to lymphoid chemokines. *J. Exp. Med.* 190: 1123–1134.
27. Ozaki, K., R. Spolski, C. G. Feng, C. F. Qi, J. Cheng, A. Sher, H. C. Morse, III, C. Liu, P. L. Schwartzberg, and W. J. Leonard. 2002. A critical role for IL-21 in regulating immunoglobulin production. *Science* 298: 1630–1634.
28. Craft, J. E., R. L. Grodzicki, M. Shrestha, D. K. Fischer, M. García-Blanco, and A. C. Steere. 1984. The antibody response in Lyme disease. *Yale J. Biol. Med.* 57: 561–565.
29. Kalish, R. A., G. McHugh, J. Granquist, B. Shea, R. Ruthazer, and A. C. Steere. 2001. Persistence of immunoglobulin M or immunoglobulin G antibody responses to *Borrelia burgdorferi* 10-20 years after active Lyme disease. *Clin. Infect. Dis.* 33: 780–785.
30. Buerki, H., H. Cottier, M. W. Hess, J. Laissue, and R. D. Stoner. 1974. Distinctive medullary and germinal center proliferative patterns in mouse lymph nodes after regional primary and secondary stimulation with tetanus toxoid. *J. Immunol.* 112: 1961–1970.
31. Sealy, R., S. Surman, J. L. Hurwitz, and C. Coleclough. 2003. Antibody response to influenza infection of mice: different patterns for glycoprotein and nucleocapsid antigens. *Immunology* 108: 431–439.
32. Pereira, J. P., L. M. Kelly, and J. G. Cyster. 2010. Finding the right niche: B-cell migration in the early phases of T-dependent antibody responses. *Int. Immunol.* 22: 413–419.
33. Cyster, J. G. 2005. Chemokines, sphingosine-1-phosphate, and cell migration in secondary lymphoid organs. *Annu. Rev. Immunol.* 23: 127–159.
34. Narayan, K., D. Dail, L. Li, D. Cadavid, S. Amrute, P. Fitzgerald-Bocarsly, and A. R. Pachner. 2005. The nervous system as ectopic germinal center: CXCL13 and IgG in lyme neuroborreliosis. *Ann. Neurol.* 57: 813–823.
35. Barthold, S. W., M. S. de Souza, J. L. Janotka, A. L. Smith, and D. H. Persing. 1993. Chronic Lyme borreliosis in the laboratory mouse. *Am. J. Pathol.* 143: 959–971.
36. Vora, K. A., L. C. Wang, S. P. Rao, Z. Y. Liu, G. R. Majeau, A. H. Cutler, P. S. Hochman, M. L. Scott, and S. L. Kalled. 2003. Cutting edge: germinal centers formed in the absence of B cell-activating factor belonging to the TNF family exhibit impaired maturation and function. *J. Immunol.* 171: 547–551.
37. Diamond, M. S., B. Shrestha, E. Mehlhop, E. Sitati, and M. Engle. 2003. Innate and adaptive immune responses determine protection against disseminated infection by West Nile encephalitis virus. *Viral Immunol.* 16: 259–278.
38. Schulze, R. J., and W. R. Zückert. 2006. *Borrelia burgdorferi* lipoproteins are secreted to the outer surface by default. *Mol. Microbiol.* 59: 1473–1484.
39. Stoenner, H. G., T. Dodd, and C. Larsen. 1982. Antigenic variation of *Borrelia* hermsii. *J. Exp. Med.* 156: 1297–1311.
40. Barthold, S. W. 1993. Antigenic stability of *Borrelia burgdorferi* during chronic infections of immunocompetent mice. *Infect. Immun.* 61: 4955–4961.
41. Baumgarth, N., O. C. Herman, G. C. Jager, L. E. Brown, L. A. Herzenberg, and J. Chen. 2000. B-1 and B-2 cell-derived immunoglobulin M antibodies are nonredundant components of the protective response to influenza virus infection. *J. Exp. Med.* 192: 271–280.
42. Racine, R., M. McLaughlin, D. D. Jones, S. T. Wittmer, K. C. MacNamara, D. L. Woodland, and G. M. Winslow. 2011. IgM production by bone marrow plasmablasts contributes to long-term protection against intracellular bacterial infection. *J. Immunol.* 186: 1011–1021.
43. Foote, J. B., T. I. Mahmoud, A. M. Vale, and J. F. Kearney. 2012. Long-term maintenance of polysaccharide-specific antibodies by IgM-secreting cells. *J. Immunol.* 188: 57–67.
44. Taillardet, M., G. Haffar, P. Mondière, M. J. Asensio, H. Gheit, N. Burdin, T. Defrance, and L. Genestier. 2009. The thymus-independent immunity conferred by a pneumococcal polysaccharide is mediated by long-lived plasma cells. *Blood* 114: 4432–4440.
45. Diamond, M. S., E. M. Sitati, L. D. Friend, S. Higgs, B. Shrestha, and M. Engle. 2003. A critical role for induced IgM in the protection against West Nile virus infection. *J. Exp. Med.* 198: 1853–1862.
46. Tobita, T., M. Oda, and T. Azuma. 2004. Segmental flexibility and avidity of IgM in the interaction of polyvalent antigens. *Mol. Immunol.* 40: 803–811.
47. Belperron, A. A., C. M. Dailey, C. J. Booth, and L. K. Bockenstedt. 2007. Marginal zone B-cell depletion impairs murine host defense against *Borrelia burgdorferi* infection. *Infect. Immun.* 75: 3354–3360.
48. de Souza, M. S., A. L. Smith, D. S. Beck, L. J. Kim, G. M. Hansen, Jr., and S. W. Barthold. 1993. Variant responses of mice to *Borrelia burgdorferi* depending on the site of intradermal inoculation. *Infect. Immun.* 61: 4493–4497.
49. Baumgarth, N. 2011. The double life of a B-1 cell: self-reactivity selects for protective effector functions. *Nat. Rev. Immunol.* 11: 34–46.
50. Alugupalli, K. R., R. M. Gerstein, J. Chen, E. Szomolanyi-Tsuda, R. T. Woodland, and J. M. Leong. 2003. The resolution of relapsing fever borreliosis requires IgM and is concurrent with expansion of B1b lymphocytes. *J. Immunol.* 170: 3819–3827.
51. Alugupalli, K. R., J. M. Leong, R. T. Woodland, M. Muramatsu, T. Honjo, and R. M. Gerstein. 2004. B1b lymphocytes confer T cell-independent long-lasting immunity. *Immunity* 21: 379–390.
52. Cariappa, A., I. B. Mazo, C. Chase, H. N. Shi, H. Liu, Q. Li, H. Rose, H. Leung, B. J. Cherayil, P. Russell, et al. 2005. Perisinusoidal B cells in the bone marrow participate in T-independent responses to blood-borne microbes. *Immunity* 23: 397–407.
53. Müllegger, R. R., T. K. Means, J. J. Shin, M. Lee, K. L. Jones, L. J. Glickstein, A. D. Luster, and A. C. Steere. 2007. Chemokine signatures in the skin disorders of Lyme borreliosis in Europe: predominance of CXCL9 and CXCL10 in erythema migrans and acrodermatitis and CXCL13 in lymphocytoma. *Infect. Immun.* 75: 4621–4628.
54. Golde, W. T., B. Robinson-Dunn, M. G. Stobierski, D. Dykhuizen, I. N. Wang, V. Carlson, H. Stiefel, S. Shiflett, and G. L. Campbell. 1998. Culture-confirmed reinfection of a person with different strains of *Borrelia burgdorferi* sensu stricto. *J. Clin. Microbiol.* 36: 1015–1019.